

Effects of Molecular Weights of Bioabsorbable Poly(*p*-dioxanone) on its Crystallization Behaviors

Ke-Ke Yang, Xiu-Li Wang, Yu-Zhong Wang, Hai-Xia Huang

Center for Degradable and Flame-Retardant Polymeric Materials, College of Chemistry, Sichuan University, Chengdu 610064, People's Republic of China

Received 11 November 2004; accepted 30 June 2005

DOI 10.1002/app.23003

Published online in Wiley InterScience (www.interscience.wiley.com).

ABSTRACT: The crystallization behaviors of poly(*p*-dioxanone) (PPDO) with different molecular weights (MWs) have been studied using a differential scanning calorimetry. The results showed that the MW of PPDO affects the crystallization rate and crystallinity obviously during the dynamic crystallization process. The Avrami equation has been used to analyze the overall isothermal crystallization of PPDO. Avrami exponents ranging from 2 to 3 were obtained with good fits (correlation coefficients were greater than

0.999 in all the cases) at T_c ranged from 55 to 75°C. Although no significant influence of MW on Avrami exponent has been found, the MW of PPDO plays dominant role on the rate constant k . The values of k increase with the MW in a T_c range from 55 to 75°C. © 2006 Wiley Periodicals, Inc. *J Appl Polym Sci* 100: 2331–2335, 2006

Key words: poly(*p*-dioxanone); crystallization behavior; DSC; molecular weight

INTRODUCTION

Poly(*p*-dioxanone) {poly(1,4-dioxan-2-one), PPDO} is a kind of material with outstanding biodegradability, bioabsorbability, biocompatibility, and good flexibility,¹ and is well known as a good candidate for medical use. In 1970s, PPDO has been applied to produce absorbable monofilament suture PDS by Ethicon Inc. More applications in the medical field, such as bone or tissue fixation device and drug delivery system, were also reported frequently in the recent years.^{2–7} Furthermore, PPDO also has great potential for general uses such as films, molded products, laminates, foams, nonwoven materials, adhesives, and coatings.⁸ However, PPDO has not attracted interest because the polymerization of the PPDO is not an easy work. Until recently, more attention has been paid on the synthesis of PPDO.^{9–14} The researches on properties and modification of PPDO begin to flourish.^{15–24} Our research group has synthesized a series of PPDO

with different molecular weights (MWs) that bring great convenience for the further research of PPDO.

As a crystalline polyester, the crystallization behavior of PPDO is a very important character, which became the research focus in a short time. Sabino et al.¹⁵ studied the crystallization and morphology of PPDO suture (PDS), using polarized optical microscopy (PM) and differential scanning calorimetry (DSC). The equilibrium melting point was determined to be 127°C. The Avrami exponents were found to range from 3 to 4 as isothermal crystallization temperature increased from 50 to 100°C. Furthermore, Andjelic et al.¹⁶ studied both isothermal crystallization and nonisothermal crystallization of PDS and dyed PDS. Pezzin et al.¹⁷ also used PDS as the object to study the melt behavior, crystallinity, and morphology. The equilibrium melting temperature was determined at 114°C. MW is one of the key factors, which not only governed the thermodynamic and kinetic parameters of polymer crystallization but also influenced the equilibrium melting point, crystal thickness, crystallization kinetics, degree of crystallinity, and crystalline morphology. The aim of this article is to deal with this issue by using PPDO with different MWs synthesized via the same method in our laboratory.

Correspondence to: Y.-Z. Wang (yzwang@mail.sc.cninfo.net).

Contract grant sponsor: The Ministry of Education of China (the Excellent Talent Program and Young Teachers Program).

Contract grant sponsor: National Natural Science Foundation of China; contract grant number: 50303012.

Contract grant sponsor: 863 Program; contract grant number: 2002AA322030.

Contract grant sponsor: Key Project of International Cooperation of China; contract grant number: 2004DFA04700.

EXPERIMENTAL

Materials

PPDO was synthesized by bulk polymerization of *p*-dioxanone (PDO), which was provided by the Center for Degradable and Flame-Retardant Polymeric Mate-

rials (Chengdu, China) and was dried before use. Ring-opening polymerization of *p*-dioxanone was performed with magnetic stirring in flame-dried glass reactors. The reactors were evacuated and purged with argon several times prior to addition of PDO and stannous octoate catalyst solution with a syringe (the mole ratio of PDO monomer and stannous octoate is 15,000:1). Then, the reactors were immersed into a silicone oil bath kept at 80°C for predetermined intervals. The reactors were rapidly cooled down to room temperature, and the products were purified by precipitation from the phenol/1,1,2,2-tetrachloroethane (2:3 w/w) solution with methanol and dried under vacuum to a constant weight.

As the conventional solvents such as chloroform, tetrahydrofuran, and toluene used in GPC measurements cannot resolve PPDO with high MWs, only the viscosity-average MWs of the resulting polymers were measured in phenol/1,1,2,2-tetrachloroethane (2:3 w/w) solution using an Ubbelohde viscosimeter thermostated at 25°C. The MWs of PPDO can be calculated from the intrinsic viscosity $[\eta]$ according to Mark-Houwink equation $[\eta] = KM_v^\alpha$, where $\alpha = 0.63$ and $K = 79 \times 10^{-3} \text{ cm}^3/\text{g}$ (Table I).¹⁵ Therefore, the information of MW distribution cannot be supplied in the present work.

Differential scanning calorimetry

Dynamic crystallization of PPDO

Thermal analysis was performed with a SEIKO EXSTAR60000 DSC. Samples were first heated to 140°C for 5 min to erase all previous thermal history, then were cooled to -50°C at rate of 10°C/min, and then were heated to 140°C at the same rate. Both the cooling scan and heating scan have been recorded for the analysis.

Isothermal crystallization of PPDO

Samples were first heated to 140°C for 5 min to erase all previous thermal history and were then quenched at a rate of 80°C/min to the required isothermal crystallization temperature (T_c). The sample was held at T_c

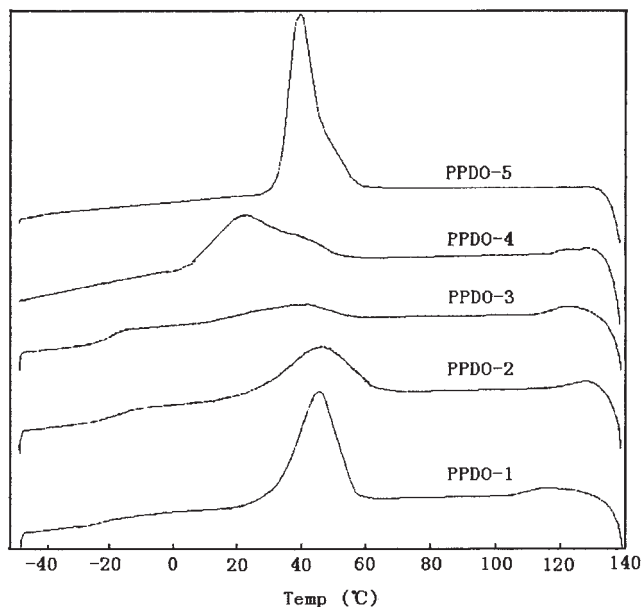


Figure 1 DSC cooling scan of PPDO with different inherent viscosity at 10°C/min after erasing thermal history at 140°C for 5 min.

for enough time to develop the maximum possible crystallinity degree.

RESULTS AND DISCUSSION

Dynamic crystallization of PPDO

Figures 1 and 2 illustrate the cooling and heating scan of PPDO with different MWs. The relevant data derived from Figures 1 and 2 were tabulated in Table II. After the same scanning procedure, the five PPDO samples showed different results. PPDO-1 and PPDO-5, the samples with highest MW and lowest MW, developed the fully possible crystallinity during cooling scan (Fig. 1), and no crystallization behavior has been found in the following heating scan (Fig. 2). The absolute crystallinities of PPDO-1 and PPDO-5 were 40.0 and 43.5%, respectively, (Table II). (The heat of fusion ΔH_m^0 for 100% crystalline PPDO has been determined by Wunderlich and coworkers²⁵ as 14.4kJ/mol). Otherwise, the rest of the three samples exhibited different behaviors: the endothermic peaks appeared both in cooling scan and heating scan in the curves of PPDO-2, PPDO-3, and PPDO-4. To differentiate the crystallization proportion in the first and second scans, we introduced the conception of relative crystallinity and deemed the total crystallization after the whole scan procedure as 100%. The data derived of all the samples are listed in Table II. In detail, the relative crystallinities were 100, 71.3, 30.6, 87.5, and 100% in the cooling scan and 0, 28.7, 69.4, 12.5, and 0% in the heating scan for PPDO-1, PPDO-2, PPDO-3, PPDO-4, and PPDO-5, respectively.

TABLE I
Viscosity Average Molecular Weight of PPDO Samples

Sample	\bar{M}_v^a (10^4 g/mol)
PPDO-1	18.78
PPDO-2	8.54
PPDO-3	4.77
PPDO-4	2.20
PPDO-5	0.27

^a \bar{M}_v was calculated from Mark-Houwink equation $[\eta] = KM_v^\alpha$, where $\alpha = 0.63$ and $K = 79 \times 10^{-3} \text{ cm}^3/\text{g}$.¹⁵

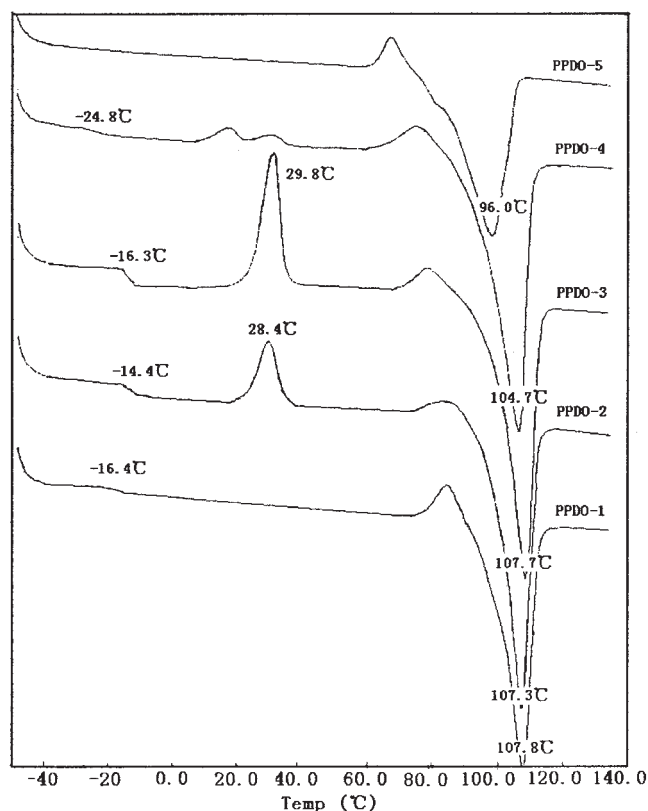


Figure 2 DSC heating scan of PPDO with different inherent viscosity after the cooling scan shown in Figure 1.

It is well known that there are two key factors that control the overall crystallization rate, one is the nucleation and the other is the crystal.^{26,27} The MW of polymer affects these two factors on significant level. The nucleation of polymer has been found to be an increasing function of the MW of polymer, but the crystal varies with MW in an opposite way.²⁸ Furthermore, both these factors are temperature-dependent. Nucleation is a decreasing function of temperature; however, crystal is an increasing function of temper-

ature.^{27,28} Moreover, the crystallization of PPDO samples was a dynamic process in this case, and so the scanning procedure (first the cooling scan, followed by heating scan) and the scanning rate will also influence the crystallization behavior. The former determined the crystallization process of all PPDO samples, which should begin with a temperature-dropping process and then a temperature-rising process; the latter determined the interval of time, in which the samples stay in a suitable crystallization temperature range. The combination of all those factors may result in the aforementioned crystallization behaviors of PPDO.

The effect of MW acted not only on the crystallization behavior but also on the glass transition temperature (T_g) to a certain extent. In very low MW range, T_g is an increasing function of MW, but the MW of polymers will no longer affect T_g if it is higher than the critical value. In this work, T_g of PPDO-1, PPDO-2, and PPDO-3 with higher MW are very close, -16 through -14°C , but T_g of PPDO-4 with lower MW is found at -24.8°C , much lower than the aforementioned three samples. Moreover, no glass transition has been found in the programmed temperature range of PPDO-5 due to its extremely low MW (Fig. 2). On the other hand, the T_g transition also displayed some information of crystallinity of PPDO. The glass transition of PPDO-2 was more obvious compared with that of PPDO-1 (Fig. 2), which is related to the crystallinity of those two samples. The absolute crystallinity of PPDO-1 reached 40.0% (Table II) after the first cooling scan, and the fraction of amorphous region is about 60%. However, the absolute crystallinity of PPDO-2 is 24.5% after the first cooling scan, and 75.5% amorphous region in the sample is left. It is evident that the fraction of amorphous region of PPDO-2 is greater than that of PPDO-1, and therefore its glass transition is more clear than PPDO-1. Similarly, this phenomenon could be found in PPDO-3 and PPDO-4 (Fig. 2).

TABLE II
Relevant Data Derived from Figures 1 and 2

	PPDO-1	PPDO-2	PPDO-3	PPDO-4	PPDO-5
T_{c1}					
T_{c1} ($^\circ\text{C}$)	46.1	46.0	45.0	22.9	40.3
ΔH (J/g)	-56.46	-34.62	-14.84	-43.31	-61.46
$X_{c,r}$ (%)	100	71.3	30.6	87.5	100
T_{c2}					
T_{c2} ($^\circ\text{C}$)	-	28.4	29.8	-	-
ΔH (J/g)	-	-13.92	-34.06	-6.16	-
$X_{c,r}$ (%)	0	28.7	69.4	12.5	0
$X_{c,a}$ (%)	40.0	34.4	34.6	35.0	43.5
T_g ($^\circ\text{C}$)	-16.4	-14.4	-16.3	-24.8	-
T_m ($^\circ\text{C}$)	107.8	107.3	107.7	104.7	96.0

$X_{c,r}$, relative crystallinity; and $X_{c,a}$, absolute crystallinity.

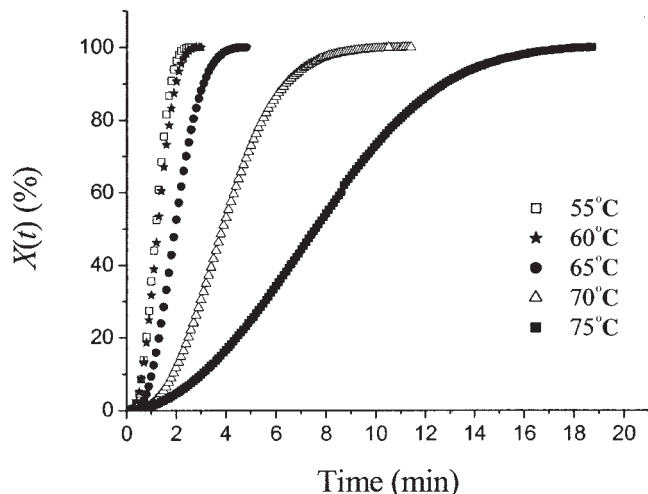


Figure 3 Relative crystalline fraction *versus* time at different isothermal crystallization temperature for PPDO-1.

Isothermal crystallization of PPDO

In this case, three samples of PPDO with different MW, PPDO-1, PPDO-2, and PPDO-4, have been chosen to investigate the influence of the MW on the kinetic parameters of PPDO crystallization. Isothermal crystallization was carried out at five different temperatures 55, 60, 65, 70, and 75°C, respectively. Figure 3 illustrates the typical plots of relative crystalline fraction versus crystallization time for PPDO-1. PPDO-2 and PPDO-4 have the same trend and is not shown here. The figure showed that the higher T_c , the longer crystallization time is needed in this temperature range. If $t_{1/2}$ is used to express the time in which 50% crystalline has been finished, then $\tau_{1/2}$ ($\tau_{1/2} = (t_{1/2})^{-1}$) can be used to express the crystallization rate.^{27,29} The calculated data manifest that the crystallization rate is a decreasing function of T_c ranged from 55 to 75°C (Fig. 4). The influence of MW was also evident. In most cases, the higher the MW of sample, the faster is the crystallization rate. In detail, the values of $\tau_{1/2}$ are 0.016, 0.012, and 0.0076 s⁻¹ at 55°C for PPDO-1, PPDO-2, and PPDO-4, respectively. In other words, $\tau_{1/2}$ of PPDO-1 is 1.33 time faster than PPDO-2 and 2.11 time than PPDO-4.

Avrami's equation^{26-27,29} has been utilized to analyze the isothermal crystallization data obtained by DSC.

$$1 - X(t) = \exp(-kt^n)$$

where n is the Avrami exponent, k is the rate constant, and $X(t)$ is the relative crystalline fraction of the polymer. The logarithmic form of it can be given as follows

$$\log[-\ln(1-X(t))] = \log k + n \log t$$

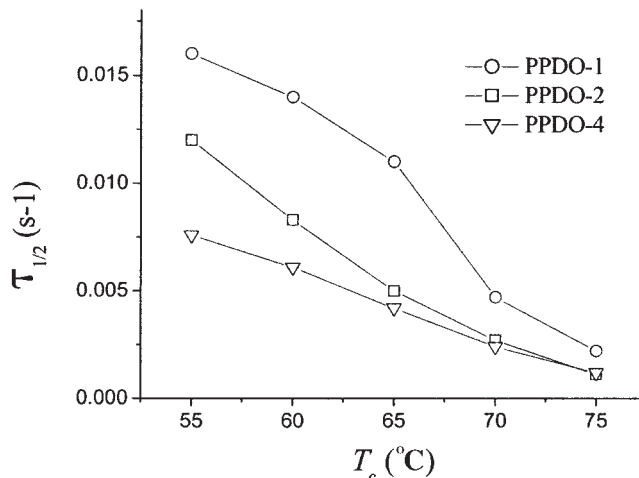


Figure 4 $\tau_{1/2}$ as a function of T_c .

From this equation, it is an easy work to obtain values of n for various crystallization temperatures by plotting $\log t$ against $\log[-\ln(1-X(t))]$.

Figure 5 shows typical isothermal Avrami plots for PPDO-1. PPDO-2 and PPDO-4 have the same trend and is not shown here. It is well known that Avrami equation works well in the primary crystallization range, and divergence appears when the secondary crystallization occurs.^{15,26-27} On a significant level, the value of n was found to be dependent on the conversion degree range selected. In the present work, a conversion range from 0 to 65% has been chosen, and very good fits have been obtained. In detail, correlation coefficients were greater than 0.999 in all the cases. The values of n and k derived from the Avrami analysis for the samples are tabulated in Table III. Here, all values of n range from 2 to 3, and the mean values of Avrami exponents for PPDO-1, PPDO-2, and PPDO-4 are 2.34, 2.28, and 2.28, respectively. Appar-

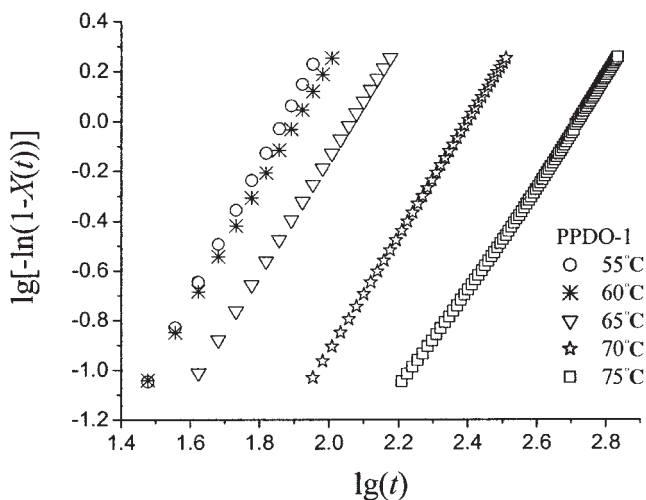


Figure 5 Avrami curve for PPDO-1.

TABLE III
Relevant Data of Avrami Curves for PPDO

Sample	T_c (°C)	k (s^{-n})	n
PPDO-1	55	1.07×10^{-5}	2.66
	60	2.34×10^{-5}	2.43
	65	1.91×10^{-5}	2.29
	70	2.82×10^{-6}	2.21
	75	1.82×10^{-6}	2.11
PPDO-2	55	1.48×10^{-5}	2.42
	60	1.02×10^{-5}	2.32
	65	2.57×10^{-6}	2.35
	70	2.08×10^{-6}	2.15
	75	2.69×10^{-7}	2.16
PPDO-4	55	4.57×10^{-6}	2.45
	60	2.95×10^{-6}	2.43
	65	2.75×10^{-6}	2.27
	70	8.51×10^{-7}	2.25
	75	9.77×10^{-7}	2.00

ently, the MW of PPDO has no significant influence on the values of Avrami exponent (Table III). In other words, the spherulitic morphology of PPDO is independent of the MW. Furthermore, it indicates the nucleation growth of the PPDO samples in this condition, following a two-dimensional discs growth mechanism. Otherwise, all these three samples (PPDO-1, PPDO-2, and PPDO-4) exhibited the same trend that is the slight decrease in Avrami exponent with increase of T_c . However, the influences of T_c or MW on the values of k are distinct. In one hand, k is a decreasing function of T_c ranged from 55 to 75°C for all samples in most cases. In other hand, k is an increasing function of MW in most cases. It agrees quite well with the results obtained earlier. In recent literature,¹⁶ T_{max} of PPDO at the maximum rate has been found at 45°C, and so the T_c chosen in this case are greater than T_{max} . It is well known that the overall crystallization rate is a decreasing function of T_c in this range.²⁶ Furthermore, the growth rate of nucleation acts dominant role of the overall crystallization rate in this range of T_c and the growth rate of nucleation increases with the MW. Then, it is undoubting that the overall crystallization rate increases with the MW of PPDO.

CONCLUSIONS

The investigation in present work suggests that the MW of PPDO plays a very important role not only in dynamic crystallization process but also in isothermal crystallization process. In dynamic crystallization process of PPDO, the DSC curves vary with MW. The MW of PPDO influences both crystallization growth rate and the crystallinity.

The Avrami equation has been applied to analyze the isothermal crystallization behavior. Avrami exponents ranged from 2 to 3 were obtained with good fits at T_c ranged from 55 to 75°C. Although no significant influence of MW on Avrami exponent has been found, the MW of PPDO plays dominant role on the rate constant k . The values of k increase with the MW in a T_c range between 55 and 75°C.

References

1. Yang, K. K.; Wang, X. L.; Wang, Y. Z. *J Macromol Sci Polym Rev* 2002, C42, 373.
2. Gertzman, A.; Thompson, D. R. U.S. Pat. 4,591,630 (1986).
3. Cachia, V. V.; Juan, M. S. U.S. Pat. 5,893,850 (1999).
4. Mattei, F. V.; Doddi, N. U. S. Pat. 4,440,789 (1984).
5. Song, C. X.; Sun, H. F.; Feng, X. D. *Polym J* 1987, 19, 485.
6. Zhu, K. J.; Lin, X. Z.; Yang, S. L. *J Appl Polym Sci* 1990, 39, 1.
7. Li, X. W.; Xiao, J.; Li, X. Y.; Xiong, C. D.; Deng, X. M. *Polym Mater Sci Eng* 1998, 14, 20 (Chinese).
8. PCT Int. Appl. WO 9,721,753 A1 (1997).
9. Kricheldorf, H. R.; Damrau, D. O. *Macromol Chem Phys* 1998, 199, 1089.
10. Wang, H.; Dong, J. H.; Qiu, K. Y. *Acta Polym Sin* 1997, 6, 319 (Chinese).
11. Nishida, H.; Yamoshita, M.; Endo, T.; Tokiwa, Y. *Macromolecules* 2000, 33, 6982.
12. Raquez, J. M.; Degee, Ph.; Narayan, R.; Dubois, Ph. *Macromol Rapid Commun* 2000, 21, 1063.
13. Raquez, J. M.; Degee, Ph.; Narayan, R.; Dubois, Ph. *Macromolecules* 2001, 34, 8419.
14. Yang, K. K.; Wang, X. L.; Wang, Y. Z. Presented at Symposium on Polymers, Zhengzhou, China, Oct. 12–16 2001.
15. Sabino, M. A.; Feijoo, J. L.; Müller, A. *J Macromol Chem Phys* 2000, 201, 2687.
16. Andjelic, S.; Jamiolkowski, D.; Mcdivitt, J.; Fischer, J.; Zhou, J.; Vetrecin, R. *J Appl Polym Sci* 2001, 79, 742.
17. Pezzin, A. P. T.; Alberda van Ekenstein, G. O. R.; Duck, E. A. R. *Polymer* 2001, 42, 8303.
18. Sabino, M. A.; Feijoo, J. L.; Müller, A. *J Polym Degrad Stab* 2001, 73, 541.
19. von Fraunhofer, J. A.; Storey, R. S.; Stone, I. K.; Masterson, B. J. *J Biomed Mater Res* 1985, 19, 595.
20. Andjelic, S.; Jamiolkowski, D.; Mcdivitt, J.; Fischer, J.; Zhou, J.; Wang, Z. G.; Hsiao, B. S. *J Polym Sci Part B: Polym Phys* 2001, 39, 152.
21. Andjelic, S.; Fitz, B. D. *J Polym Sci Part B: Polym Phys* 2000, 38, 2436.
22. Wang, X. L.; Yang, K. K.; Wang, Y. Z. *Acta Materialia* 2004, 52, 4899.
23. Wang, X. L.; Yang, K. K.; Wang, Y. Z. *J Polym Sci Part A: Polym Chem* 2004, 42, 3417.
24. Wang, X. L.; Yang, K. K.; Wang, Y. Z. *Polymer* 2004, 45, 7961.
25. Ishikiriya, K.; Pyda, M.; Zhang, G.; Forschner, T.; Grebowicz, J.; Wunderlich, B. *J Macromol Sci Phys* 1998, B37, 27.
26. Ma, D. Z.; He, P. S.; Xu, Z. D.; Zhou, L. Q. Structures and properties of polymer; Scientific Press: Beijing, 1999.
27. Yin, J. H.; Muo, Z. S. Modern Polymeric Physics; Science Press: Beijing, 2001.
28. Chen, H. L.; Li, L. J.; Ou-Yang, W. C.; Hwang, J. C.; Wong, W. Y. *Macromolecules* 1997, 30, 1718.
29. Liu, Z. H.; Hatakeyama, T.; Chen, X. S. Calorimetric Analysis of Polymer; Press of Chemical Engineering: Beijing, 2002.